DETERMINATION OF THE OPTIMUM COMBINATION OF PARAMETERS OF SPECIALIZED BLADES FOR THE SHANTUI SD 32 BULLDOZER WHEN MOVING LOW-DENSITY MATERIALS

Tavbay Khankelov[1,*], Maloxat Abdukadirova[2], Otabek Ochildiev[3], Zebo Alimova[4], Gulxayo Niyazova[4], Anvar Kadirov[5]

[1]Department of Engineering of Technological Machines, Tashkent State Transport University (TSTU), Tashkent, Uzbekistan
[2]Department of Ecology and Water Resources Management, Tashkent Institute of Irrigation and Agricultural Mechanization Engineers, National Research University, Tashkent, Uzbekistan
[3]Departments of Health, Safety and Environment, Termez Institute of Engineering and Technology, Termez, Uzbekistan
[4]Department of Transport Power Plants, Tashkent State Transport University (TSTU), Tashkent, Uzbekistan
[5]Department of Applied Mechanics, Tashkent State Transport University (TSTU), Tashkent, Uzbekistan

*E-mail of corresponding author: xankelovt9@gmail.com

Tavbay Khankelov 0000-0002-4653-4679, Maloxat Abdukadirova 0000-0003-1188-2662,
Otabek Ochidiev 0000-0002-9573-5979, Zebo Alimova 0000-0002-6711-5318,
Gulxayo Niyazova 0009-0008-8673-0560, Anvar Kadirov 0000-0002-9773-7249

Resume

Recommendations are given on combinations of parameters of box-shaped and “dump” types of dumps for the SHANTUI SD 32 bulldozer, which provide the highest technical characteristics of the bulldozer when moving low-density materials. The optimal dimensions of a box blade for equipping the SHANTUI SD32 bulldozer are a grasp width of up to 3730 mm, radius of curvature of up to 1700 mm, width of the cutting edge of up to 460 mm, canopy width of up to 140 mm, flap length of up to 860 mm. The optimal dimensions of a “landfill” blade for equipping the SHANTUI SD32 bulldozer are a grasp width of up to 3900 mm, radius of curvature of up to 460 mm, width of the cutting edge of up to 124 mm, canopy width of up to 610 mm.

Article info

Received 10 February 2025
Accepted 14 April 2025
Online 10 June 2025

Keywords:
dozing prism
technical performance
box blade
“landfill” blade
material
efficiency,
optimization

Available online: https://doi.org/10.26552/com.C.2025.042

ISSN 1335-4205 (print version)
ISSN 2585-7878 (online version)

1 Introduction

Bulldozers are widely used in construction. Currently, there are about as many of them in operation as there are excavators. Bulldozers account for about 35-40% of the total volume of earthworks performed in construction. Bulldozers work in road-building, reclamation, irrigation, construction, and in quarries of the mining industry. They carry out leveling work, constructing road and railway embankments from lateral reserves, transporting soil over a distance of up to 100 m, digging canals and pits, filling trenches and holes, clearing roads and construction sites of snow, felling trees and uprooting stumps. They are used as pushers when working with scrapers [1]. It is known that there are materials (snow, wood chips, coal, etc.), which in some cases are most convenient to move with bulldozers, but the capacities of blades designed for working with soils do not ensure full use of the machine traction and power. For such situations, bulldozer blades of high capacity were developed, called specialized blades. For this study, the term “specialized blades” refers to bulldozer blade-type working bodies of high capacity, for which the large-scale excavation is neither the only nor primary nor the preferred area of application. These include [2]: U-dozer blades for moving light materials, box blades for moving light, bulk, liquefied and coarse materials, “landfill” blades for moving household waste. The work is devoted to finding the optimal combination of blade parameters for the SHANTUI SD 32 bulldozer. Mathematical modelling of the working process of a bulldozer was taken as a research method, and the technical performance of the bulldozer was chosen as a criterion for the quality of blade parameters, providing a reliable assessment of the results of parametric synthesis of blades [3].

2 Literature sources review and problem statement

Many structural, technological, and ergonomic factors influence the performance of a bulldozer. In addition, some researchers in their works also take into account the position that with the maximum set of the soil drag prism in front of the dump, its area of contact with the frontal surface is determined by the position of the dump in the cross section determined by the chip formation trajectory of the soil layer [4]. For example, in [5-7], the issues of the influence of the cutters' design and the properties of materials on the performance of a bulldozer were studied, and losses from the dozing prism were taken into account only by introducing a loss factor. In [8-10], formulas for determining the productivity consider not only the design but the technological parameters of a bulldozer, as well. It should be noted that some publications [11-15] also take into account the driver's qualifications by introducing a correction factor. Issues related to the calculation of the main parameters of earth-moving machines are addressed in [16-19]. References [20-23] take into account the influence of developed areas' properties on the efficiency of the digging, leveling, and transportation processes. Currently, a large number of studies [24-31] are devoted to the issues of automation of work processes, unmanned control of earthmoving equipment, and the influence of unmanned control on the efficiency of machines. Despite the numerous studies aimed at determining the performance of a bulldozer, the issues of considering the losses of transported materials from the dozing prism and choosing the optimal combination of bulldozer blades based on the properties of the transported materials, are relevant.

3 Purpose and objectives of the study

In the structure of generalized indices assessing the efficiency of the road-building machines (mainly, energy and mass indices), productivity occupies a special place. Performance evaluation provides a basis for assessing the suitability of a machine for its functional purpose. To find the optimal combination of parameters of box and "landfill" types of blades for the SHANTUI SD 32 bulldozer when developing various materials of reduced density and cohesion that provide the greatest technical performance. To achieve this goal, the following tasks were solved:

- establishing the patterns of the processes of prism formation, considering their discrete phases;
- development of a mathematical model of the performance of a bulldozer equipped with any type of blade, considering the losses from the dozing prism;
- classification and quantitative description of probable production situations;
- development of recommendations for combinations of parameters of the box and "landfill" types of blades for the SHANTUI SD 32 bulldozer.

3.1 The process of prism formation considering the losses

For this study, the maximum volume of material that can be removed by a blade is considered as the blade capacity.

Analysis of the relationships proposed in [4-12] for determining the capacity of the blade made it possibly to conclude [18] that the formula proposed by Balovnev et al. [1] and the model proposed by Karasev et al. [19,] are the closest to the generally accepted concepts about the mechanism of prism formation, experimental data and the objectives of this study. The disadvantage of the former is that it describes the maximum volume of the dozing prism, while, in reality, the performance of the bulldozer depends on the level of losses from the dozing prism during its formation and movement. Below is outlined the methodology for considering such losses when calculating the dozing capacity.

4 Materials and methods

It is accepted that the material being moved can either be stored in heaps or presented as a layer along the ground line.

When moving a pile (a heap) of material, losses begin from the time when the entire volume of material captured by the blade begins to move along the ground line, i.e. when the formation of the dozing prism is completed. Here:

$$Q = Q_{\max}, \tag{1}$$

where Q is the dozing capacity, m^3; Q_{max} is the maximum value of the dozing capacity, m^3.

The current value of the dozing capacity is

$$Q_i = Q_{i-1} + dQ, \tag{2}$$

where Q_i is the dozing capacity Q at the end of the i-th section of the bulldozer path of dl_t length, m^3; Q_{i-1} is the dozing capacity Q at the beginning of the i-th section of the bulldozer path of length dl_t, m^3; dQ is the capacity of loosened material entering the dozing prism on the i-th section of the bulldozer path of length dl_t, m^3.

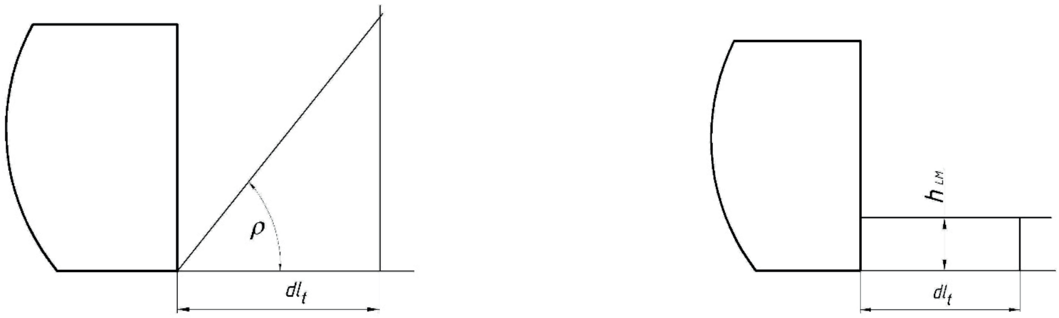

a) b)

Figure 1 *Volume of material entering the dozing prism: a) when collecting from a heap; b) during the layered cutting, where ρ is the angle of natural repose of material;* dl_t *is the incremental step length of the bulldozer path, mm;* h_{LM} *is the thickness of the layer of material cut by the blade, mm*

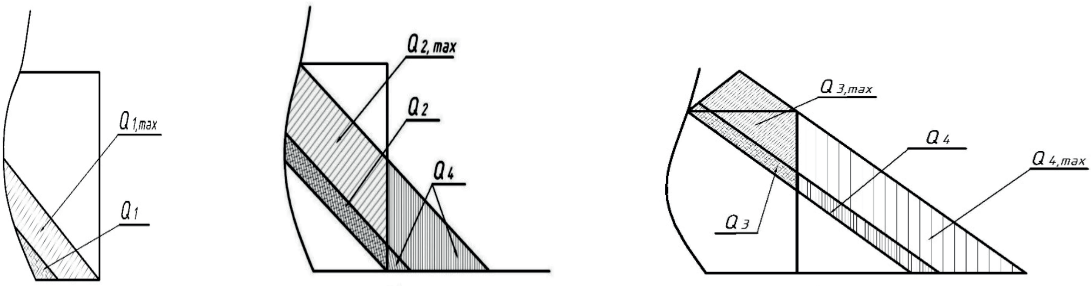

a) b) c)

Figure 2 *Phases of dozing prism formation: a) 1st phase; b) 2nd phase; c) 3rd phase*

$$dQ = (i - 0.5) \cdot dl_t^2 \cdot tg\rho \cdot L \cdot f_r \text{, (Figure1),} \quad (3)$$

where dl_t is the incremental step length of the bulldozer, m; $(i - 0.5)$ is the represents a coefficient that determines the amount of material entering the drag prism; $tg\rho$ is the tangent of the angle of inclination of the drag prism; ρ is the angle of natural repose of the material, degree; L is the grasp width of the blade, m; f_r is the loosening coefficient of the material. The volume of material entering the dozing prism is shown in Figure 1.

When forming a dozing prism from a layer of material, it is assumed that the process goes through three phases (Figure 2).

Phase 1 - the dozing prism grows from zero to capacity $Q_{1,max}$ due to the growth of component Q_1. (Figure 2, a); there are no losses from the dozing prism;

Phase 2 - the dozing prism grows from capacity $Q_{1,max}$ to ($Q_{1,max}$ + $Q_{2,max}$ + Q_4) due to the growth of components Q_2 and Q_4 (Figure 2, b); the volume of losses is proportional to capacity Q_4;

Phase 3 – the dozing prism grows from capacity ($Q_{1,max}$+ $Q_{2,max}$ + Q_4) to due to the growth of components Q_3 and Q_4 (Figure 2, c); the volume of losses is proportional to capacity Q_4; where Q_1,Q_2,Q_3,Q_4 are the components of the dozing prism, m^3; $Q_{1,max}$,$Q_{2,max}$,$Q_{3,max}$,$Q_{4,max}$ are the maximum values of capacities Q_1,Q_2,Q_3,Q_4 respectively.

The phase ends with the end of the growth of the dozing prism. For the current value of dozing capacity Q, the following is true:

$$Q_i = Q_{i-1} + dQ - Q_L, \quad (4)$$

(Figure 1, b): Q_L is the volume of losses on the i-th section of the bulldozer path of dl_t, m^3 long.

$$dQ = h_{LM} \cdot L \cdot dl_t \cdot f_r, \quad (5)$$

where f_r is the loosening coefficient of the material.

The proportionality of losses to the part of dozing capacity that is not limited on the sides by the blade flaps (Q_4 in Figure 2) is expressed by the following formula:

$$Q_L = Q_4 \cdot K_L \cdot dl_t, \quad (6)$$

where K_L is the loss coefficient from the dozing prism. Thus, the task of considering losses from a dozing prism when calculating its capacity comes down to determining the value of Q_4 in discrete sections of the bulldozer path from the point of the beginning of prism formation to the point of its completion. Along this path, the pattern of the volume formation process will change at points (Figure 2) corresponding to the following boundary conditions:

$$Q_1 = Q_{1,\max} \quad (7)$$

is the beginning of the process of Q_4 formation (volume Q_4 forms as soon as Q_1 reaches its maximum value,

$$Q_2 = Q_{2,\max} \quad (8)$$

is the change in the pattern of Q_4 formation (pattern of Q_4 formation changes as soon as Q_2 reaches its maximum value),

$$Q_3 = Q_{3,\max} \quad (9)$$

is the end of the dozing prism growth process (the dozing prism growth stops as soon as Q_3 reaches its maximum value).

Another condition for stopping the growth of the dozing prism is that the losses are equal to the volume of material entering the blade:

$$Q_L = dQ. \quad (10)$$

Moreover, the condition in Equation (10) takes precedence over condition in Equation (9), because when it occurs, the growth of the dozing prism stops, although Q_3 has not yet reached its maximum value.

4.1 Dozing capacity considering the losses

According to the accepted assumptions and corresponding boundary conditions in Equations (7)-(10), design schemes shown in Figures 3-6 were taken for calculating capacities Q_1, $Q_{1,max}$, Q_2, $Q_{2,max}$, Q_3, $Q_{3,max}$, Q_4 and $Q_{4,max}$. To simplify the analysis, the cylindrical surfaces of the blade sections were replaced by vertical planes. In the final determination of the dozing capacity, the allowed error was corrected by adding to the prism the capacity proportional to the part of the segment formed by the surface of the blade and the vertical plane (Figure 3).

$$Q_{me} = (F_1 + F_2)[L + 2W(1 - \cos\mu)], \quad (11)$$

$$F_1 = 0.5R^2(\alpha - \sin\alpha), \quad (12)$$

$$F_1 = \frac{H}{2}\sqrt{\begin{bmatrix}2(1-\cos\alpha)+\\+k_a^2+2k_a\cdot\sin\alpha\end{bmatrix}R^2 - H_0^2}, \quad (13)$$

$$H_0 = H/[1 + k_b\cdot\sin(\alpha+\gamma+\delta)], \quad (14)$$

where F_1, F_2 are the cross-sectional areas of cylindrical segments, m^2; R is the radius of curvature of the cross profile of the blade, m; H is the height of the blade with a canopy, m; k_α is the ratio of the width of the cutting edge to the radius of curvature; k_b is the ratio of the width of the canopy to the radius of curvature; H_0 is the height of the blade without canopy, m.

Checking the fulfillment of condition in Equation (7) involves calculating the maximum capacity value (Figure 4).

$$Q_{1,\max} = W^2\sin^2\mu\cdot tg\rho\begin{bmatrix}(L-2W\cos\mu)/\\2+(2W\sin\mu/3)\end{bmatrix} \quad (15)$$

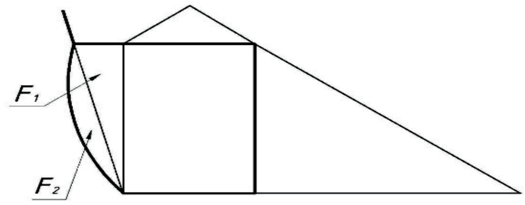

Figure 3 *Additional volume formed by the curvature of the blade and its digging angle inclination*

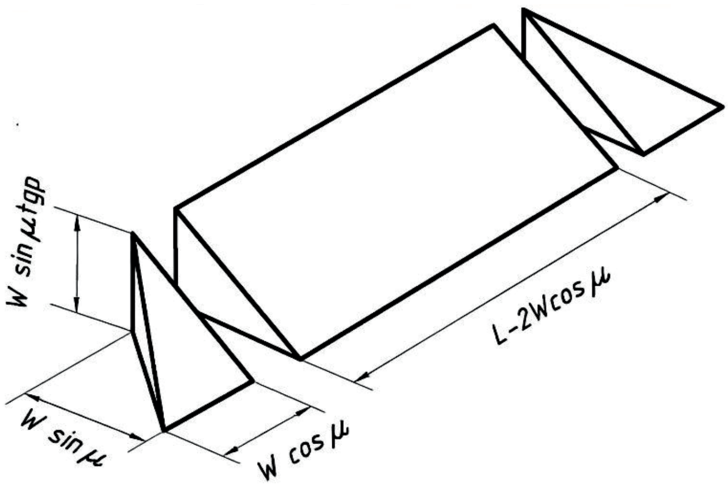

Figure 4. *Scheme for calculating the volume of a drawing prism at the end of the 1st phase of its growth*

In the second phase of filling the blade, the dozing prism grows due to Q_2 and Q_4 related by the following equation:

$$Q_{2,i} + Q_{4,i} = Q_{2,(i-1)} + Q_{4,(i-1)} + dQ. \tag{16}$$

From which follows:

$$dQ_2 + dQ_4 = dQ, \tag{17}$$

$$dQ_2 = Q_{2,i} - Q_{2,(i-1)}, \tag{18}$$

$$dQ_4 = Q_{4,i} - Q_{4,(i-1)}, \tag{19}$$

From the design diagram (Figure 5), it follows that:

$$dQ_2 = W\sin\mu(L - W\cos\mu)dz_2, \tag{20}$$

$$dQ_4 = L \cdot dz_2 \cdot (2z_2 + dz_2)/2tg\rho, \tag{21}$$

$$dz_2 = \left[-c_2 + \sqrt{(c_2^2 + 4b_2dQ)}\right]/2b_2 \tag{22}$$

$$b_2 = L/2tg\rho, \tag{23}$$

$$c_2 = (L - W\cos\mu)W\sin\mu + z_2L/tg\rho, \tag{24}$$

$$z_{2,i} = z_{2,(i-1)} + dz_2, \tag{25}$$

where dz_2 is the projection of the layer thickness dQ_2 onto the OZ vertical axis; z_2 is the projection of the layer thickness Q_2 onto the OZ vertical axis.

Q_2 and Q_4 are calculated by the following formulas:

$$Q_{2i} = Q_{2(i-1)} + dQ_2, \tag{26}$$

$$Q_{4,i} = Q_{4(i-1)} + dQ_4. \tag{27}$$

Checking condition is

$$Q_2 \leq Q_{2,\max}, \tag{28}$$

where:

$$Q_{2,\max} = (H - W\sin\mu tg\rho) \cdot W \cdot \sin\mu \cdot (L - W\cos\mu), \tag{29}$$

In the third phase of filling the blade, the dozing prism increases due to Q_3 and Q_4 (Figure 2, c), related by:

$$Q_{3,i} + Q_{4,i} = Q_{3(i-1)} + Q_{4(i-1)} + dQ. \tag{30}$$

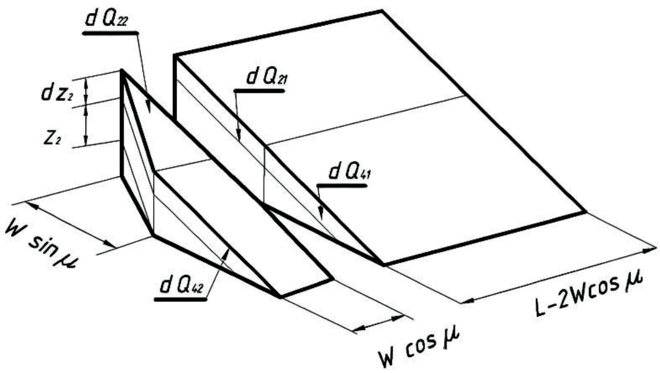

Figure 5 *Scheme for calculating the capacities that determine the growth of the dozing prism in the second phase*

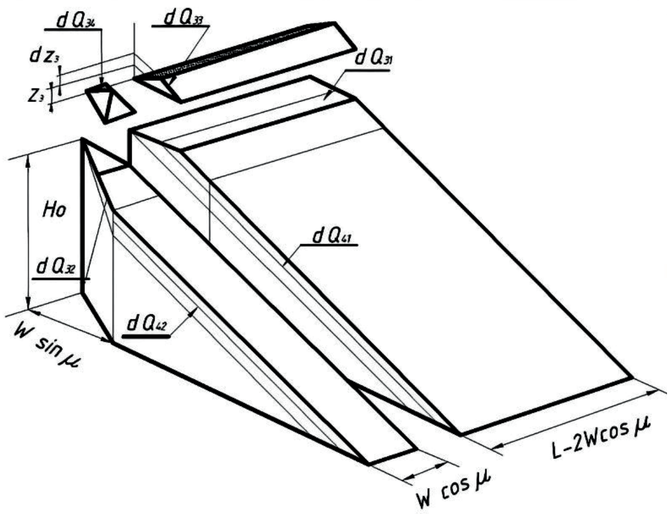

Figure 6 *Scheme for calculating the capacities that determine the growth of the dozing prism in the third phase*

From which follows:

$$dQ_3 + dQ_4 = dQ\,, \tag{31}$$

$$dQ_3 = Q_{3,i} - Q_{3(i-1)}\,, \tag{32}$$

$$dQ_4 = Q_{4,i} - Q_{4(i-1)}\,. \tag{33}$$

Calculation schemes of the capacities that determine the growth of dozing prisms in the second and third phases are shown in Figures 5 and 6.

From the calculation scheme in Figure 6, it follows that

$$dQ_3 = a_3 dz_3^3 + (b_3 - L/2tg\rho)dz_3^2 + \\ +(c_3 - L(z_2 + z_3)/)dz_3, \tag{34}$$

$$dQ_4 = (L/2tg\rho)dz_3^2 + (L(z_2 + z_3)/tg\rho)dz_3\,. \tag{35}$$

The value of dz_3 is found from the following equation:

$$a_3 dz_3^3 + b_3 dz_3^2 + c_3 dz_3 = dQ\,, \tag{36}$$

$$a_3 = -1/(6tg^2\rho tg\mu)\,, \tag{37}$$

$$b_3 = z_3/(2tg^2\rho \cdot tg\mu) + (L - 2W\cos\mu)\cdot \\ \cdot z_3/(2tg\rho) + L/2tg\rho, \tag{38}$$

$$c_3 = z_3^2/2tg^2\rho \cdot tg\mu + (L - 2W\cos\mu)z_3/2tg\rho + \\ +(L - 2W\cos\mu)z_3/2tg\rho + (L - 2W\cos\mu)\times \\ \times W\sin\mu + L(z_2 + z_3)/tg\rho \tag{39}$$

$$z_{3,i} = z_{3(i-1)} + dz_3\,, \tag{40}$$

Q_3 and Q_4 are calculated by the following formulas:

$$Q_{3,i} = Q_{3(i-1)} + dQ_3\,, \tag{41}$$

$$Q_{4,i} = Q_{4(i-1)} + dQ_4\,, \tag{42}$$

checking conditions are

$$Q_3 \leq Q_{3,\max} \text{ and } Q_4 \leq Q_{4,\max}\,, \tag{43}$$

where:

$$Q_{3,\max} = (W\sin^2\mu)tg\rho(3L - 4W\cos\mu)/4\,, \tag{44}$$

$$Q_{4,\max} = H_0^2 L/2tg\rho\,, \tag{45}$$

For the path traveled by the blade, at any point in the current section it is equal to

$$l_{t,i} = l_{t,(i-1)} + dl_t\,, \tag{46}$$

4.2 Nomenclature and characteristics of the removed materials

In accordance with the technical specifications, the materials for which specialized blades are intended to be processed include packed snow, municipal solid waste, liquefied soil, wood chips. Physical properties of these materials, characterizing them as removed media and ground line, were established by analysis of literary sources [21-24] and are summarized in Table 1.

4.3 Technological options for performing work with specialized blades

Analysis of probable options for using specialized blades made it possible to classify and quantitatively describe several cases characterized by a standard set of parameters:

1. Moving the heap without cutting and without distributing it at the end of the passage.
2. Moving the heap with cutting, without distributing it as a layer at the end of the passage.

***Table 1** Physical properties of materials*

Properties of materials	Packed snow	Municipal waste	Liquified soil	Wood chips
Cohesion index*	1	1	2	1
Coefficients:				
Metal friction	0.06	0.55	0.13	0.4
Material friction	0.51	1.00	0.18	1.05
Loosening the material	1.2	1.4	1.0	1.2
Resistance to motion	0.1	0.12	0.1	0.12
a_u	0.05	0.05	0.05	0.05
b_u	1.76	1.76	1.76	1.76
n	12	8	12	8
Cutting resistance, kN/m^2	21.6	20.0	17.8	30.0
Angle of repose, degrees	60	55	10	50
Volumetric mass, t/m^3	0.40	0.43	1.8	0.35

*1- cohesive material, 2- non-cohesive material

3. Moving the heap without cutting, distributing it as a layer at the end of the passage.
4. Collecting a dozing prism by cutting without distributing it as a layer at the end of the passage.
5. Collecting a dozing prism by cutting, distributing it as a layer at the end of the passage.
6. Moving the heap without cutting, distributing it along the length of the passage.

The values of parameters characterizing technological options for using specialized blades are given in Table 2.

5 Results

5.1. Bulldozer performance when calculating blade capacity using the T. Khankelov model

Below tables 3, 4, 5 and 6 present the results of calculations of bulldozers‘ performance equipped with specialized blades Straight blade, Half U-dozer, U-dozer, Box-blade, Landfill blade when developing the following materials, such as Packed snow, Municipal solid waste, Liquefied soil, Wood chips for the main technological variants of works presented in paragraph 4.3.

Table 2 *Characteristics of technological options*

Properties characterizing the option	Technological option					
	1	2	3	4	5	6
Allowable maximum slipping, %	100	100	100	100	100	100
Thickness of the material layer to be removed, m	0.0	0.2	0.2	0.2	0.2	0.0
Layer of leveling material, m	0.0	0.3	0.3	0.0	0.3	0.3
Total length of the machine‘s working stroke, m	80	80	80	80	80	80
Time for auxiliary operations, s	26	26	26	26	26	26
Blade position at*:						
collection	2	2	2	3	3	2
displacement	2	3	3	3	3	3
unloading	0	0	1	0	1	1

*0 - no operation, 1 - the blade does not touch the surface, 2 - the blade is in a “floating” position, 3 - the blade is pressed to the surface

Table 3 *Bulldozer capacity for packed snow, m^3/h*

Technology option number	1	2	3	4	5	6
Straight blade	232	208	207	203	202	233
Half U-dozer	236	208	206	201	208	242
U-dozer	240	207	211	199	200	238
Box blade	225	210	210	202	205	233
Landfill blade	362	315	313	317	317	371

Table 4 *Bulldozer capacity for municipal solid waste, m^3/h*

Technology option number	1	2	3	4	5	6
Straight blade	223	192	191	192	198	224
Half U-dozer	221	195	192	199	197	221
U-dozer	225	195	192	197	197	220
Box blade	226	194	197	194	194	221
Landfill blade	312	279	273	275	279	323

Table 5 *Bulldozer capacity for liquefied soil, m^3/h*

Technology option number	1	2	3	4	5	6
Straight blade	622	598	609	569	594	624
Half U-dozer	621	598	601	558	618	633
U-dozer	615	613	611	568	588	617
Box blade	615	620	612	576	605	633
Landfill blade	363	331	329	322	329	365

Table 7 presents the results of calculations of 6-hour and 48-hour total output of bulldozers equipped with specialized blades Straight blade, Half U-dozer, U-dozer, Box-blade, Landfill blade at the development of the above-mentioned materials under the main technological options.

5.2. Bulldozer performance when calculating blade capacity according to G. N. Karasev

Tables 8, 9, 10 and 11 below present the results of calculations of bulldozer productivity of bulldozers equipped with specialized blades Straight blade, Half U-dozer, U-dozer, Box-blade, Landfill blade when developing the following materials Packed snow, Municipal solid waste, Liquefied soil, Wood chips for the main technological variants of works presented in section 4.3.

Table 12 presents the results of calculations of 6-hour and 48-hour total output of bulldozers equipped with specialized blades Straight blade, Half U-dozer, U-dozer, Box-blade, Landfill blade at development of the above-mentioned materials under the main technological variants.

6 Discussion of results

By assuming an equal probability of bulldozer operation under different operating conditions, it is possible to compare blades in terms of their total output. The total output for 6 hours (Tables 7 and 12) is the sum of the hourly productivity of the bulldozer, calculated for one material and each of the 6 technological options. For example, number 1285 in Table 7 (straight blade, material No. 1) is the sum of numbers from the “straight blade” line of Table 3 (packed snow).

Table 6 *Bulldozer capacity for wood chips, m^3/h*

Technology option number	1	2	3	4	5	6
Straight blade	259	216	214	213	218	252
Half U-dozer	253	216	217	212	215	254
U-dozer	253	214	219	208	216	252
Box blade	255	217	216	209	217	250
Landfill blade	356	304	304	306	307	369

Table 7 *Total output, m^3*

In 6 hours					
Number of material	1	2	3	4	In 48 hours
Blades:	1285	1220	3616	1372	7493
Straight					
Half U-dozer	1301	1225	3629	1367	7522
U-dozer	1295	1228	3612	1362	7497
Box	1285	1226	3661	1364	7536
Landfill	1995	1741	2039	1946	7721

Table 8 *Bulldozer capacity for packed snow, m^3/h*

Technology option number	1	2	3	4	5	6
Straight blade m3/h	286	247	246	247	250	288
Half U-dozer, m3/h	283	250	251	247	251	280
U-dozer, m3/h	277	245	246	240	243	281
Box blade, m3/h	282	250	251	243	246	284
Landfill blade, m3/h	492	445	450	438	441	491

Table 9 *Bulldozer capacity for municipal solid waste, m^3/h*

Technology option number	1	2	3	4	5	6
Straight blade m3/h	278	250	249	247	244	278
Half U-dozer, m3/h	278	253	254	244	252	272
U-dozer, m3/h	273	252	248	244	253	275
Box blade, m3/h	274	255	252	249	252	284
Landfill blade, m3/h	424	389	399	380	392	430

Table 10 *Bulldozer capacity for liquefied soil, m³/h*

Technology option number	1	2	3	4	5	6
Straight blade m3/h	785	961	952	734	955	990
Half U-dozer, m3/h	785	956	967	735	962	999
U-dozer, m3/h	784	964	948	736	960	998
Box blade, m3/h	785	962	957	733	954	994
Landfill blade, m3/h	779	965	959	736	954	918

Table 11 *Bulldozer capacity for wood chips, m³/h*

Technology option number	1	2	3	4	5	6
Straight blade m3/h	334	285	285	279	285	336
Half U-dozer, m3/h	337	291	284	288	279	291
U-dozer, m3/h	336	291	287	276	283	340
Box blade, m3/h	332	284	290	281	289	341
Landfill blade, m3/h	507	473	488	452	475	518

Table 12 *Total output, m³*

	In 6 hours				
Number of material	1	2	3	4	In 48 hours
Blades:	1564	1546	5377	1804	9291
Straight					
Half U-dozer	1562	1553	5404	1770	10289
U-dozer	1532	1545	5390	1813	9280
Box	1980	1566	5385	1817	9748
Landfill	2757	2414	4352	2913	12436

The total output for 6 hours indicates that regardless of operating conditions (except for liquefied soil) and the method of calculating the blade capacity, the best performance for a bulldozer is provided by a straight blade with an enlarged lattice canopy (the so-called “landfill”). When working with liquefied soil, the greatest productivity is achieved using a box blade.

The total output for 48 hours (i.e., the sum of the hourly productivity of the bulldozer for all materials and for all technological options), assuming the equal probability of the bulldozer operation with any materials according to any technological options, indicates (see Tables 7 and 12) that the greatest efficiency can be expected from a bulldozer equipped with a “landfill” type of a blade. The next largest total output, which is 16-24% less (depending on the method of calculating the blade capacity) is provided by a box blade. The outputs of straight, half U-dozer, and U-dozer blades differ slightly (by 0.2% regardless of the method of calculating the blade capacity), which indicates their approximately equal efficiency under the operating conditions considered. Thus, we can conclude that given the equal probability of the considered operating conditions, the greatest efficiency is ensured by equipping the bulldozer with a “landfill” type of blade, and when operating predominantly with liquefied soil, cement concrete mortars, and other such materials, the greatest efficiency is ensured by a box blade.

The feasibility of installing one of the two types of blades on a bulldozer is determined by the probability of its operating on a particular material since the total output of a bulldozer over a fixed time is a probabilistic value:

$$C_{48} = \sum (C_{6i} \cdot p_i), \quad (47)$$

where C_{48} is the total output of the bulldozer in 48 hours using all materials and all technological options, m³; C_{6i} is the total output of the bulldozer for 6 hours on the i-th material for all technological options, m³; p_i is the probability of the bulldozer operating on the i-th material; i is the number of the material for which the output is calculated.

If we assume an equal probability of bulldozer operation for any technological options on any material (except the liquefied soil), then from the data in Tables 3, 7, and 12, it follows that the box blade and the “landfill” blade provide the same total output of the bulldozer; while for its operation on liquefied soil (or similar materials) total output is from 0.27 to 0.5 depending on the method of calculating the blade capacity. If there is a greater probability of the bulldozer operating

Table 13 *Optimized dimensions of a box blade*

Optimized blade parameter		Liquefied soil
Grasp width, m	according to Khankelov	3.83-3.93
	according to Karasev	3.55-3.73
Radius of curvature, m	according to Khankelov	1.58-1.66
	according to Karasev	1.43-1.70
The ratio of the flap length to the grasp width	according to Khankelov	0.22-0.23
	according to Karasev	0.22-0.23

Table 14 *Optimized parameters of a "landfill" blade*

Optimized parameters of a blade		Snow, waste
Grasp width, m	according to Khankelov	3.77-3.92
	according to Karasev	3.63-3.90
Radius of curvature, m	according to Khankelov	0.44-0.46
	according to Karasev	0.41-0.62

on liquefied soil, the high output will be ensured by installing a box blade, and if the probability is less - by installing a "landfill" blade. The dimensions of the box and "landfill" blades optimized for operating with the corresponding materials are given in Tables 13 and 14.

It follows from the data that, depending on the method of calculating the blade capacity, the ranges of optimal values for its dimensions can vary significantly. In particular, this applies to a box blade; its ranges of the grasp width and radius of curvature, calculated by different methods do not overlap (Table 13). In principle, experimental testing of each calculated model to determine the most correct one can eliminate this discrepancy. The difficulties of such testing due to material and financial costs are obvious, and the unambiguity of its results (as evidenced by many years of experience in experimental research) is not guaranteed. Therefore, for practical purposes, authors can recommend:

a) for a box blade:
- set the grasp width to no more than 3750 mm to prevent a possible decrease in bulldozer performance due to increased slippage;
- set the curvature radius to no more than 1700 mm so as not to limit the view from the bulldozer driver's cab;
- set the cutting edge width to no more than 460 mm;
- set the canopy width to no more than 140 mm;
- set the flap length to no more than 860 mm.

b) for a "landfill" blade:
- take the grasp width in the range of 3770-3900 mm;
- take the radius of curvature in the range of 440-460 mm;
- take the width of the cutting edge in the range of 118-124 mm;
- take the width of the canopy in the range of 580-610 mm.

7 Conclusion and future work

An analysis of the effectiveness of equipping the SHANTUI SD32 bulldozer with specialized high-capacity blades showed that the work of the bulldozer on materials that differ in their characteristics from ordinary loamy soil (snow, household waste, liquefied soil, coal, wood chips) could be performed with the highest productivity using the box and "landfill" blades. Moreover, the performance feasibility is determined by the probability of the bulldozer operating on liquefied soil (or similar materials) or other materials (snow, waste, coal, wood chips). The undeniable effectiveness of equipping a bulldozer with a box blade is expected when the probability of the machine operating on liquefied soil (or similar materials) is 0.5 or more.

The optimal dimensions of a box blade for equipping the SHANTUI SD32 bulldozer are a grasp width of up to 3730 mm, radius of curvature of up to 1700 mm, cutting edge width of up to 460 mm, canopy width of up to 140 mm, flap length up to 860 mm. The optimal dimensions of a "landfill" blade for equipping the SHANTUI SD32 bulldozer are a grasp width of up to 3900 mm, radius of curvature of up to 460 mm, cutting edge width of up to 124 mm, canopy width of up to 610 mm. Future work may be aimed at introducing artificial intelligence into the development of various materials with lower specific gravity. Provided that the developed mathematical models are supplemented with parameters describing their properties, as well as the operating conditions of the machines, it will be possible to significantly increase the efficiency of these machines with the least energy and material costs.

Acknowledgements

The authors received no financial support for the research, authorship and/or publication of this article.

Conflicts of interest

The authors declare that they have no known competing financial interests or personal relationships that could have appeared to influence the work reported in this paper.

References

[1] BALOVNEV, V., GLAGOLEV, S., DANILOV, R., KUSTAREV, G., SHESTOPALOV, K., GERASIMOV, M. *Machines for excavation work: design, calculation, consumer properties*. Minsk: BSTU Publishing House, 2012. ISBN 978-985-525-899-6.

[2] DUDKIN, M., KIM, A., AUKENOVA, B., RADENKOV, R., SAVELIEV, A., ANDRYUKHOV, N. Theoretical investigations of the process of interaction with environment of a bulldozer blade with variable geometry. *Journal of Applied Engineering Science* [online]. 2022, **20**(3), p. 798-807. ISSN 1451-4117, eISSN 1821-3197. Available from: https://doi.org/10.5937/jaes0-37210

[3] ASLONOV, N., IRISOV, K. Mathematical model of resistance to spreading forces using a bulldozer blade. *E3S Web of Conferences* [online]. 2023, **390**, 01032. eISSN 2267-1242A. Available from: https://doi.org/10.1051/e3sconf/202339001032

[4] SURASHOV, N., ASMATULLAEV, R., TOLYMBEK, D. Determination of the rational shape of a bulldozer blade, taking into account the soil background of the Republic of Kazakhstan. *Bulletin of SibADI* [online]. 2021,**18**(6), p. 662-677. ISSN 2071-7296, eISSN 2658-5626. Available from: https://doi.org/10.26518/2071-7296-2021-18-6-662-677

[5] KHMARA, L. Scientific support of construction and road machines: research, calculation, creation, selection, use. *Bulletin of the Pre-Dnieper State Academy of Construction and Architecture*. 2019, **209**(7-8), p. 48-69. ISSN 2312-2676.

[6] RAKSHA, S., GLAVATSKY, K., GREBENKO, Y. Study of the process of digging soil with a physical model of bulldozer equipment with a fixed blade and a replaceable blade system. *Bulletin of the Kharkov National Automobile and Highway University* [online]. 2020, **88**(2), p. 86-92. ISSN 2219-5548, eISSN 2521-1773. Available from: https://doi.org/10.30977/BUL.2219-5548.2020.88.2.86

[7] SELECH, J., ULBRICH, D., WLODARCZYK, K., STASZAK, Z., MARCINKIEWICZ, J., RAMEK, D., BARAN, B. A working design of a bulldozer blade as additional equipment of a compaction drum roller. *MATEC Web of Conferences* [online]. 2019, **254**, 04005. eISSN 2261-236X. Available from: https://doi.org/10.1051/matecconf/201925404005

[8] BARAKAT, N., SHARMA, D. Evolutionary multi-objective optimization for bulldozer and its blade in soil cutting. *International Journal of Management Science and Engineering Management* [online]. 2019, **12**(4), p. 102-112. ISSN 1750-9653, eISSN 1750-9661. Available from: https://doi.org/10.1080/17509653.2018.1500953

[9] KHANKELOV, T., ASKARKHODZAEV, T., ASLANOV, N. Modeling of segmental excavator working tool for soil compaction. *E3S Web of Conferences* [online]. 2023, **401**, 826. eISSN 2267-1242A. Available from: https://doi.org/10.1051/e3sconf/202340102052

[10] HIRAYAMA, M., GUIVANT, J., KATUPITIYA, J., WHITTY, M. Path planning for autonomous bulldozer. *Mechatronics* [online].2019, **58**, p. 20-38. ISSN 0957-4158, eISSN 1873-4006. Available from: https://doi.org/10.1016/j.mechatronics.2019.01.001

[11] KIM, S. K., LEE, Y. S., SUN, D. I., LEE, S. K., YU, B. H., JANG, S. H., KIM, W., HAN, C. S. Development of bulldozer sensor system for estimating the position of blade cutting edge. *Automation in Construction* [online]. 2019, **106**, 102890. ISSN 0926-5805, eISSN 1872-7891. Available from: https://doi.org/10.1016/j.autcon.2019.102890

[12] KHANKELOV, T. Results of experimental studies of the process of sorting elastic components of municipal solid waste. *Academic Journal of Manufacturing Engineering*. 2021, **19**(4), p. 97-102. ISSN 1583-7904, eISSN 2601-3045.

[13] KHANKELOV, T., ASKARHODZHAEV, T., MUKHAMEDOVA, N. Determination of key parameters of a device for sorting municipal solid waste. *Journal of Critical Reviews* [online]. 2020, **7**, p. 27-28. eISSN 2394-5125. Available from: https://doi.org/10.31838/jcr.07.04.07

[14] NAVON, R., GOLDSCHMIDT, E., SHPATNISKY, Y. A concept proving prototype of automated earthmoving control. *Automation in Construction* [online]. 2003, **13**(2), p. 225-239. ISSN 0926-5805, eISSN 1872-7891. Available from: https://doi.org/10.1016/j.autcon.2003.08.002

[15] FERNANDO, A., CHEEIN, A., GUIVANT, J. SLAM-based incremental convex hull processing approach for treetop volume estimation. *Computers and Electronics in Agriculture* [online]. 2014, **102**, p. 19-30. ISSN 0168-1699, eISSN 1872-7107. Available from: https://doi.org/10.1016/j.compag.2014.01.002

[16] PENG, G., DUAN, H., TAN, Z., ZHOU, Y., LI, J., HU, B., ZHOU, CH. Construction path tracking and unmanned bulldozer. *Automation in Construction* [online]. 2023, **154**, p. 1-17. ISSN 0926-5805, eISSN 1872-7891. Available from: https://doi.org/10.1016/j.autcon.2023.105015

[17] KHANKELOV, T., AKOBIR MUKHITDINOV, A., IBROKHIMOV, S., ASLONOV, N., MIRKHOLIKOV, S. Determination of the lengths of rebounds of elastic components of solid municipal waste. *AIP Conference Proceedings* [online]. 2022, **2432**, 030028. ISSN 0094-243X, eISSN 1551-7616. Available from: https://doi.org/10.1063/5.0089528

[18] KOSIMBETOV, B., KHANKELOV, T. Usage advanced technological methods for the recovery of cone crusher equipment. *E3S Web of Conferences* [online]. 2021, **264**, 02063. eISSN 2267-1242A. Available from: https://doi.org/10.1051/e3sconf/202126402063

[19] KARASEV, G., DOTSENKO, A., KUSTAREV, G. *Machines for earthworks*. Moscow: Bastet Publishing House, 2012. ISBN 978-5-903178-28-5.

[20] KHANKELOV, T., MUKHAMEDOVA, M. Choice of garbage trucks with rational parameters according to criterion of minimum operation cycle time. *E3S Web of Conferences* [online]. 2023, **401**, 02053. eISSN 2267-1242A. Available from: https://doi.org/10.1051/e3sconf/202340102053

[21] KHANKELOV, T., SARMONOV, A., KADIROV, A. The analytical dependence of the resistance force to digging with a bulldozer blade on the main influencing factors. *E3S Web of Conferences* [online]. 2023, 458, 10001. eISSN 2267-1242A. Available from: https://doi.org/10.1051/e3sconf/202345810001

[22] KHANKELOV, T., MAKSUDOV, Z., MUKHAMEDOVA, N., TURSUNOV, S. Crushing and screening complex for the production of compost from organic components of municipal solid waste. *E3S Web of Conferences* [online]. 2021, **264**, 01026. eISSN 2267-1242A. Available from: https://doi.org/10.1051/e3sconf/202126401026

[23] KHANKELOV, T. A theory of sorting solid domestic waste. *Construction and road Mashinery*. 2001, **5**, p. 34-36. ISSN 0039-2391.

[24] TURGUMBAEV, S., KABASHEV, R. Results of experimental studies of the process of digging soils with a modernized working body under hydrostatic pressure. *Bulletin of SibADI* [online]. 2017, **2**(54), p. 36-42. ISSN 2071-7296, eISSN 2658-5626. Available from: https://doi.org/10.26518/2071-7296-2017-2(54)-36-42

[25] KHAN, S., GUIVANT, J., LI, X. Design and experimental validation of a robust model predictive control for the optimal trajectory tracking of a small-scale autonomous bulldozer. *Robotics and Autonomous System* [online]. 2022, **147**, 103903. ISSN 0921-8890, eISSN 1872-793X. Available from: https://doi.org/10.1016/j.robot.2021.103903

[26] NEZHADALI, V., ERICSSON, L. Wheel loader optimal transient in the short loading cycle. *IFAC Proceedings Volumes* [online]. 2014, **47**(3), p. 7917-7922. ISSN 1474-6670. Available from: https://doi.org/10.3182/20140824-6-ZA-1003.02419

[27] LEE, Y. S., KIM, S. H., SEO, J., HAN, J., CHANG-SOO HAN, C. S. Blade control in Cartesian space for leveling work by bulldozer. *Automation in Construction* [online]. 2020, **118**, 103264. ISSN 0926-5805, eISSN 1872-7891. Available from: https://doi.org/10.1016/j.autcon.2020.103264

[28] HARADA, J., ISHIBASHI, E. ICT bulldozer D61EXi/PXi-24 automatic dozing control improved technology. *Komatsu Technical Report*. 2018, **64**(171), p. 1-18. ISSN 1344-8641.

[29] KE, Y., LIEYUN, D., CHENG, Z., QUANLI, D., XUEPENG, W., BIN, H. 5G-bazed earthwork monitoring system for an unmanned bulldozer. *Automation in Construction* [online]. 2021, **131**, 013891. ISSN 0926-5805, eISSN 1872-7891. Available from: https://doi.org/10.1016/j.autcon.2021.103891

[30] DADHICH, S., BODIN, U., ANDERSSON, U. Key challenges in automation of earth-moving machines. *Automation in Construction* [online]. 2016, **68**, p. 212-222. ISSN 0926-5805, eISSN 1872-7891. Available from: https://doi.org/10.1016/j.autcon.2016.05.009

[31] KHANKELOV, T., RUSTAMOV, K. J., IRISBEKOVA M., SOBIROVA D. K. Substantiation of a hammer crusher for grinding municipal solid waste. *E3S Web of Conferences* [online]. 2024, 515, 03019. eISSN 2267-1242A. Available from: https://doi.org/10.1051/e3sconf/202451503019.